

## R&D ON MICRO-LOSS MONITORS FOR HIGH INTENSITY LINACS LIKE LIPAc

J. Marroncle\*, P. Abbon, A. Marchix, CEA Saclay, DRF/DSM/IRFU, Gif sur Yvette, France  
M. Pomorski, CEA Saclay, DRT/LIST/DM2I/LCD, Gif sur Yvette, France

### Abstract

Before approaching the micro-loss monitor concept, we propose to present the high intensity Linac for which the R&D program was done, LIPAc (Linear IFMIF Prototype Accelerator). This later is the feasibility accelerator demonstrator for the International Fusion Materials Irradiation Facility (IFMIF). IFMIF aims at providing a very intense neutron source ( $10^{18}$  neutron/m<sup>2</sup>/s) to test materials for the future fusion reactors. This challenging accelerator LIPAc (1.125 MW deuteron beam) is in installation progress at Rokkasho (Japan).

Then, we will focus on the feasibility study of the beam optimization inside the SRF Linac part. Commissioning of such high beam intensity has to be done with a different approach based on detection of micro-losses, CVD diamonds, set inside the cryomodule linac. This is mandatory to keep beam losses below 1W/m for hands-on maintenance purposes.

### INTRODUCTION

This paper deals with the R&D on  $\mu$ LoM (micro-Loss Monitor) which was attempted for beam fine tuning of high intensity Linac while maintaining losses below 1W/m for maintenance hands-on purpose. Beam dynamics team working on the Linear IFMIF prototype Accelerator, LIPAc, warned about the feasibility for fulfilling this requirements with the foreseen diagnostics. Thus, they proposed to introduce the new concept of beam micro-losses and required monitors for measuring them.

After a swift introduction to LIPAc and its commissioning plans, this R&D program devoted to  $\mu$ LoM will be presented. Firstly micro-loss concept will be defined, emphasizing their importance for beam optimization. Therefore the step by step study will be investigated like, counting rate estimates and their potential background contributions, experimental neutron tests for rate validation and a proposition for signal processing before to conclude.

### IFMIF CONTEXT

The International Fusion Materials Irradiation Facility (IFMIF) [1], a project involving Japan and Europe in the framework of the "Broader Approach", aims at producing an intense flux of neutrons, in order to characterize materials envisaged for future fusion reactors. This neutron source will be a combination of two deuteron beam accelerators (125 mA – 40 MeV cw) and a liquid lithium target. Therefore, these two 5 MW accelerators impinging the Li

target will produce a huge neutron flux ( $10^{18}$  neutrons/m<sup>2</sup>/s). Downstream, dedicated cells will be implemented to test the material sample responses submitted to mechanical and thermal stresses in these very harsh conditions. Shielding structures are optimized in order to roughly reproduce the neutron energy spectrum expected in fusion reactors.

IFMIF project has to face to many challenges, thus an intermediate phase of validation was decided which consists to design and built an accelerator prototype, a 1/3-scaled Li loop target and parts of test cells.

The prototype accelerator LIPAc (Linear IFMIF Prototype Accelerator) is a 1-scaled IFMIF accelerator up to the first Superconducting Radio Frequency Linac (SRF), delivering 9 MeV deuteron beam at 125 mA cw. A high beam transport line will be installed to lead safely the beam toward a high power beam dump able to handle 1.1 MW. This accelerator is in commissioning and assembling progress at Rokkasho (Japan).

### GENERAL COMMISSIONING PLANS

LIPAc accelerator components have been mainly designed and manufactured in Europe by European Institutions (CEA Saclay, CIEMAT Madrid, INFN Legnaro and SCK-CEN) under F4E management, who is also responsible of other activities. LIPAc building was constructed by QST (National institutes for Quantum and Radiological Science and Technology), who takes also in charge the supply of conventional facilities, the control system, the protection and the timing system.

The accelerating components (Fig. 1) are the injector delivering a deuteron beam at 100 keV (A), the RFQ (175 MHz) to bunch and accelerate up to 5MeV (B) and the superconductive Linac increasing the energy up to 9 MeV (C). These components are connected through beam transport lines (LEBT, MEBT, HEBT) tuned and qualified by various diagnostic monitors [2] and the beam is absorbed into the HPBD (High Power Beam Dump) (phase D) to stop safely the 1.1 MW beam power.

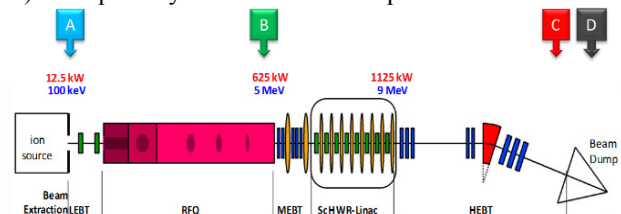


Figure 1: commission plan with the 4 phases.

\* Jacques.marroncle@cea.fr

The commissioning of the accelerator is based on a staged approach divided in 4 Phases [3].

- Phase A [4][5]: commissioning with 100 keV deuteron beam of 140 mA. Installation has already begun in 2014 for the injector and in 2015 for its commissioning. First beam was produced with  $H^+$  at the same generalized permeance, meaning half energy and half current, to keep constant the space charge effect expected for a deuteron beam, and to mitigate activation. After various proton beam measurement, injector comes to be familiar to jump to deuteron beam during 1 week. Finally, at 100 keV a 152 mA deuteron beam was extracted from the source at 10% duty cycle with  $\epsilon=0.23 \pi$ .mm.mrad; beam intensity measured on the beam stopper was about 110 mA, recently increased up to 130 mA. Encouraging results which have to be repeated this year with other condition settings.
- Phase B: installation of the RFQ [6] started in April 2016, and still in progress. In September, the bead pull measurements and the final tuning should be reached before the installation of the RFQ in its nominal position. The Mean Energy Beam Transport line [7] and a D-Plate with a low power beam dump will be attached downstream before to start the RFQ commissioning in June 2017 up to end 2017.
- Phase C and D: will resume operation after the rest of the beam line installation and the SRF Linac. Phase C commissioning concerns pulsed beam while cw will be done during phase D after the HPBD installation.

All these activities will end by December 2019.

## DEVELOPMENT OF MICRO-LOSS MONITORS FOR SRF LINACS

Beam tuning of high intensity Linacs requires a peculiar attention to beam losses which have to be kept below 1 W/m. The  $\mu$ LoMs, which should be inserted in the cryomodule, were designed to insure the SRF Linac commissioning strategy and monitoring.

As mastering the beam losses in the SRF Linac has been identified as crucial, we investigated which and how potential loss sensors could be used. After a brief SRF Linac description [8], the feasibility study of  $\mu$ LoM will be presented step by step showing that the selected system should work in this radiative environment.

### SRF Linac Description

The SRF Linac will accelerate deuteron beams from 5 to 9 MeV. It consists in one large cryostat hosting 8 identical structures, each composed of:

- 1 half wave resonator (HWR) with its own tuner for precise resonant frequency tuning, where a 175 MHz, 100 kW total RF power is injected,
- 1 solenoid equipped with steerers,
- 3 micro-loss detectors or  $\mu$ LoM around the solenoid vacuum chamber,
- 1 button BPM in front of the solenoid.

All these structures are superconductive and have their own helium vessel maintained at 4.45 K.

To protect the SRF Linac against beam losses, 8 BLMs (Beam Loss Monitor – Ion chambers LHC-type) will equipped the vacuum tank of the cryomodule.

All design, tests and procurements of the entire cryomodule including its RF couplers are done at CEA Saclay and will be completed by May 2017. Assembling of the cryomodule should start later in 2017 at Rokkasho, in a dedicated clean room, under the responsibility of F4E.

### SRF Linac Tuning And Fine Tuning

Unlike for classical accelerators where the tuning of the MEBT and the SRF Linac consists in minimizing emittance growth, for high intensity accelerators, like LIPAc, it aims at minimizing the beam external halo (the so-called "halo matching" method to decrease losses as low as  $10^{-6}$  of the beam or 1 W/m) [9]. In order to perform this matching, the necessary beam diagnostics have been identified (BPMs, BLMs and  $\mu$ LoMs) which may be implemented.

The tuning strategy relies on the principle that the number of independent diagnostics should be larger than or at least equal to the number of tuneable parameters, which are those of the MEBT quadrupoles and bunchers, together with the SRF Linac solenoids and cavities [10]. After a first dipolar tuning done with steerers aiming at minimizing trajectory deviations detected by BPMs, a quadrupolar tuning can be performed by minimizing losses detected by BLMs installed around the MEBT and the SRF Linac. As those ones are located relatively far from the beam, particle losses on the vacuum chamber would trigger several of them at once, making that the number of independent diagnostics is less than the actual number. That is why, at this step, it is foreseen to adjust only the MEBT setting, while letting the SRF Linac setting at its nominal values.

Then, in the ultimate step, referred to as fine tuning, in order to satisfy hands-on maintenance requirements, micro-losses (less than  $10^{-6}$  of the beam) detected by  $\mu$ LoM will be minimized. As those ones are close to the beam, it is expected that they are enough correlated to loss locations. In this step, all the tuneable parameters of the MEBT and the SRF Linac will be adjusted. This is necessary on the one hand, and feasible in the other hand. This has been simulated by using the Particle Swarm Optimization algorithm [11]. A fine tuning at this level of precision is expected to be made frequently, as regard to the reproducibility of the accelerator components.

### Ideal Criteria For $\mu$ LoM

We consider beam energies below few tens of MeV where only neutrons and  $\gamma$  may escape from the beam structures (pipe, cavity wall...), dictating  $\mu$ LoM choices. Hereunder is a list of requirements for such  $\mu$ LoMs:

- sensitivity to beam losses better than  $10^{-6}$  of the beam power,
- stability at cryogenic temperature since monitors are closely installed to the beam inside the cryomodule for better beam loss localizations,
- radiation tolerant,
- high counting rates because beam fine tuning is an iterative process whose effects need to be evaluated for

each single beam settings. Indeed, it requires a quite swift measurement (~1 minute per each tuning step) for achieving the final tuning in a reasonable duration time,

- reliability, like for all cryomodule components for which maintenance is a difficult and long operation,
- response to neutron better than to  $\gamma$ , as superconducting cavities may produce photons in the energy range [10 keV - few MeV]. Ideal  $\mu$ LoM should have a weak  $\gamma$  response avoiding confusion between high  $\gamma$  beam losses and  $\gamma$  cavity emission by-products,
- reasonable price.

### CVD Diamonds As $\mu$ LoM

CVD Diamonds fulfill the previous criteria but the last, thus they have been selected as the most promising sensor for  $\mu$ LoM. Main characteristics of mono crystalline CVD Diamonds are listed in the following Table 1.

Table 1: Mono Crystalline CVD Diamond Characteristics For  $\mu$ LoMs

Size	$4 \times 4 \times 0.5 \text{ mm}^3$
Active area	$3 \times 3 \text{ mm}^3$
Density	$3.52 \text{ g/cm}^3$
Resistivity	$10^{13}\text{-}10^{16} \Omega\text{m}$
$\epsilon_r$	$\sim 5.7$
e <sup>-</sup> /hole production	$\sim 13.2 \text{ eV}$
Band gap	$5.5 \text{ eV}$
Radiation hardness	$\sim 500 \text{ MRad for } 24 \text{ GeV proton}$

A thin conductive coating (Al, 200 nm) was deposited on the diamond for electric polarization (about 1V/ $\mu$ m diamond thickness). As sketched on Fig. 2, a particle may induce reactions (ionization, recoil, nuclear...) on diamond materials creating e<sup>-</sup>/hole pairs which drift toward electrodes under the electric field influence. Electric current is then measured with an appropriate electronics.

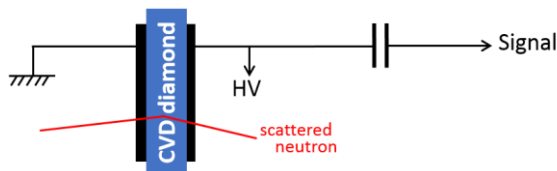


Figure 2: sketch of the diamond working principle.

### CVD Diamonds Cryogenic Tests

In 2010, no information was available about the diamond behavior at cryogenic temperature. Since diamonds will be fixed to the SRF Linac solenoids cooled at 4.5 K, characterization of crystal diamond responses at cryogenic temperature was necessary.

For this reason, cryogenic tests were done in 2 steps with a <sup>252</sup>Cf source radiating  $\gamma$  and fission neutrons bombarding diamond cooled in a liquid nitrogen Dewar (77 K) [12] in a first time, and in a liquid helium cryostat (4.5 K) in a second time [13].

For both conditions we have observed a normal diamond behavior which validates our choice allowing to resume our R&D activities about counting rate expectations.

By end 2011, it was organized a workshop on cryogenic BLM at Cern [14] where cryogenic data were available, but low  $\alpha$  particle energy exhibit anomaly which was not understood.

### Counting Rate Estimates

Expected rates for  $\gamma$  and neutrons were evaluated for of 1W/m beam losses for insuring hands-on maintenance in the SRF Linac (5 to 9 MeV). The simulated spectra (using MCNPX 2.5.0 [15]) for both incident particles shown on Fig. 3, take into account the cavity and solenoid materials of the cryomodule, while the simulated diamond responses are given on Fig. 4 for a  $3 \times 3 \text{ mm}^2$  active diamond surface. This later correspond to the conductive coating surface deposited on both sides of the diamond; at present, deposition may be extended to roughly the whole diamond surface. This is an interesting gain (16/9~2) in term of counting rates, particularly appreciated at low duty cycle beam mode.

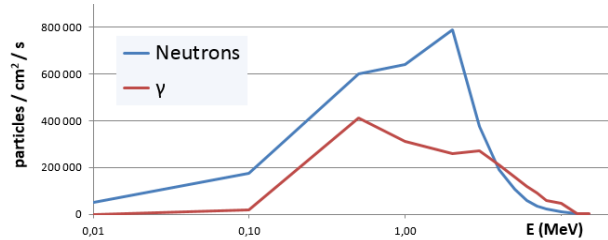


Figure 3: incident neutrons and  $\gamma$  spectra impinging diamond for SRF Linac condition for 1 W/m beam losses.

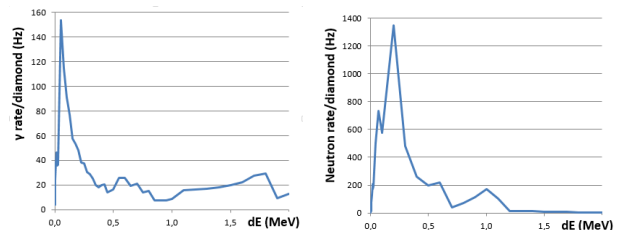


Figure 4:  $\gamma$  (left) and neutrons (right) spectra of energy deposited in diamond at SRF Linac for 1 W/m beam losses.

The 1 W/m contributions are extracted from these data for both particles and summarized on Table 2.

Table 2: Neutrons And  $\gamma$  Counting Rates (kHz) Versus Energy Thresholds (keV)

Threshold (keV)	70	100	200	300	400	500
Neutron (kHz)	3.7	3.2	1.8	1.3	1.1	0.9
Photons (kHz)	1.2	1.1	0.9	0.8	0.7	0.6

During thermal tests, we got thresholds about 50 and 100 keV, but due to the very low diamond capacitance with respect to the FEE cable length, threshold should be of the order of 200 or 300 keV!

Although the  $\mu$ LoMs are designed for full beam power, they are also expected to give wealthy indications during first tuning processes that will occur mainly at low duty cycle. Considering the extreme case of the very first commissioning phase at reduced duty cycle as low as  $10^{-4}$  leading to only 16 counts/mn for 1W/m and 200 keV threshold. These rates could actually be higher because losses in these very first phases are very likely higher than 1 W/m, and

when going to higher duty cycle  $10^{-3}$ , the counts would be hopefully multiplied by 10.

We have also checked that background contributions coming from the beam dump would represent less than 5% of the 1 W/m losses.

### $\mu$ LoM Beam Test With Neutrons

In order to validate the simulated counting rates previously presented we have tested in 2011 our  $\mu$ LoMs with various neutron energies. It was done with a Van de Graaf facility installed at CEA center of Bruyères-le-Châtel (France) which allows delivering 0.6, 0.75, 1.2, 2.1, 3.65, 6 and 16 MeV neutron beam energies using different beam / target combinations. They were produced in pulsed beam mode with a  $\gamma$  contaminations, which was efficiently discriminated by time of flight technique as seen on Fig. 5.

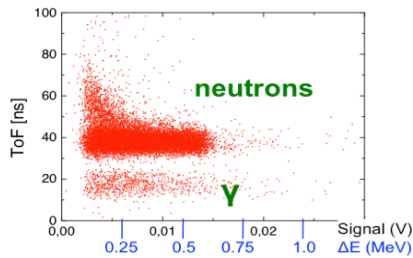


Figure 5: neutrons and  $\gamma$  time of flight discrimination for 2.1 MeV neutrons.

On Fig. 6 are plotted experimental data for  $E_{\text{neutron}} = 0.6, 0.75, 1.2$  and 2.1 MeV (dashed lines) while simulated ones are in solid lines. It clearly appears that experimental thresholds are about 100 keV. Finally, the quite good agreement between experimental and simulated data gives us a better confidence for the calculated counting rates.

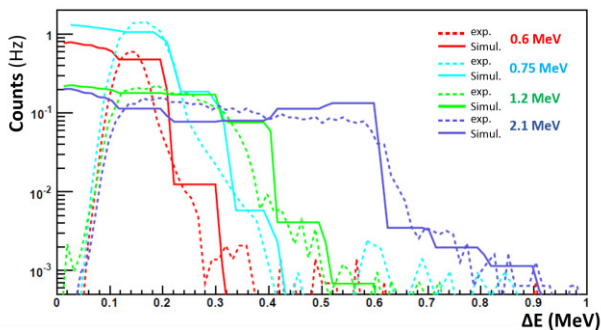


Figure 6: experimental and simulated neutron energy deposits in  $\mu$ LoM for different neutron incident energies.

### X-Rays And $\gamma$ Contaminations

As written previously, ideal  $\mu$ LoM should have a better response for neutron than for  $\gamma$ . The reason is that superconductive accelerators may emit X-rays and  $\gamma$  mainly due to high electric fields applied on the superconductive cavity surfaces. Indeed, electron emissions will generate photons when electrons impinge material. Their energies depend on electron energies, which can be strongly increased by the cavity radio frequency power when it is phase-correlated to electrons.

The goal of  $\mu$ LoM is to measure losses coming from the beam, but cryo-cavities. Since these 2 photon contributions

can't be discriminate, it is preferable to choose a photon low efficiency  $\mu$ LoM. Therefore, a low-Z material, as diamond, is a quite good candidate.

Note that the photon emission probability of superconductive cavities increases as the accelerating electric field applied: nominal value for LIPAc is 4.5 MV/m while it is 6.5 MV/m for Spiral2 for instance.

In 2013, we have set a diamond close to a cryostat inside which a Spiral2 cavity was tested. The energy deposit in the diamond was measured with an MCA (Multi-Channel Analyser). Data tacking was done at different test periods. We have noticed that generally electric field increases smoothly with low parasitic emission, but less often we have observed really important photon emissions.

This is illustrated in Table 3 where the 1 W/m is the simulated contribution of neutrons plus photons (photons are in parenthesis). The 3<sup>rd</sup> column are measured rates for normal cavity behaviour; note that the mean contribution represents less than 5% of the 1 W/m losses. This is totally different for the last column where cavity emissions are higher to the 1 W/m!

Table 3: Counting Rates (CR) At 100 And 200 keV Threshold For Superconductive Cavity Emissions

Runs	"1W/m"	few "good" runs	"bad" run
CR@Th=100 keV	4400 (1200)	203	6340
CR@Th=200 keV	2700 (1100)	77	2813

To conclude, except for specific cavity processes  $\mu$ LoM measurement should not be drawn under photon emission cavities.

### Front-End Electronics (FEE)

Preliminary study has been performed, mainly to check that adequate solution may be implemented. FEE sometimes can't be installed inside the accelerator vault due to high radiation background like for LIPAc.

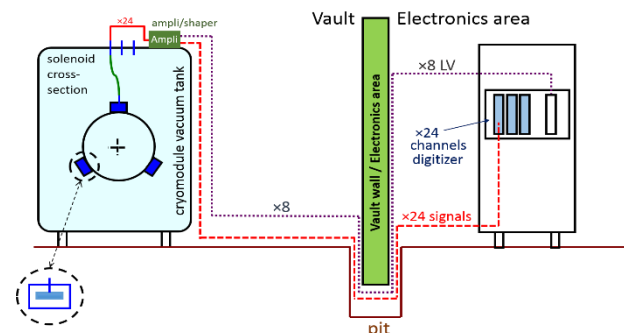


Figure 7: LIPAc vault and electronics area separated by a concrete wall for radiation shielding purpose.

However, diamond capacitance is really tiny (about 2 pF) and minimizing the cable length is of greatest importance for reducing its contribution. To keep the ratio signal/noise above a reasonable threshold, a first broadband amplifier (BW>1 GHz, Gain $\geq$ 40 dB) made of radiation tolerant components must be installed in the vault. The length of the cables connecting this amplifier to the diamond have to be minimized, but not less than 3.5 m for

LIPAc. Then, the 50  $\Omega$  output amplifier signal may be transported through a long cable to reach the second FEE level for data processing, located outside the vault (see Fig. 7).

We have measured a diamond signal with a  $^{60}\text{Co}$  source radiating 2  $\gamma$  (1.17 and 1.33 MeV). Their simulated diamond response is expected about 0.9 – 1 MeV. A broadband Cividec amplifier (BW>2 GHz – Gain=40 dB – output impedance = 50  $\Omega$  – 1 MGy radiation tolerant) [16] connected through a 3 m cable to the  $\mu\text{LoM}$  was used. Such a signal is displayed on Fig. 8.

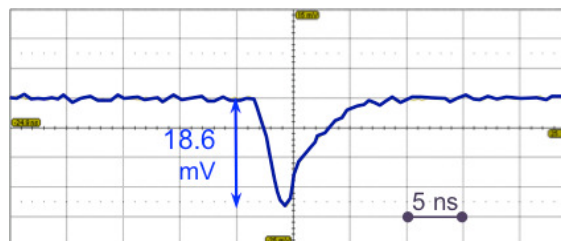


Figure 8: oscilloscope display for diamond signal submitted to a  $^{60}\text{Co}$  source.

For LIPAc, we proposed to attach 3  $\mu\text{LoMs}$  per solenoid, in order to be as close as possible to get the best loss locations. The accelerator vault is separated to the rest of the facility by a concrete wall for radiation shielding purposes.

For each  $\mu\text{LoM}$ , a radiation tolerant amplifier/shaper provides a signal which is transported to a digitizer. A CAEN digitizer as V1720 card (12 bits, 8 channels, 250 MHz sampling) [17], will process signal as soon as its amplitude is higher than a settable threshold, giving then access to the deposited charge in the  $\mu\text{LoM}$ .

During commissioning or monitoring periods, evolution of micro-losses may be followed thanks to  $\mu\text{LoM}$  which will be of great help for the machine operation group in charge of the accelerator tuning and defining working points in safe conditions.

## CONCLUSION

A R&D program about  $\mu\text{LoM}$  for beam optimization of high Linac intensity like LIPAc was initiated on IFMIF/EVEDA framework, as monitoring the very low beam losses is mandatory for achieving fine tuning.

CVD diamonds were identified as good candidates for such loss detections and deeply investigated in the frame of dedicated R&D program. This study has demonstrated how they nicely fulfil the main requirements related to radiation tolerance, operation at cryogenic temperatures, counting rates sensitivity to background particles. Thanks to the various tests performed, missing experimental values have been obtained and full characterization of the sensor for the purpose of loss measurements has been completed. A digitizing processing signal was also designed to measure the energy deposit spectra. All these elements argue for mono crystalline CVD diamond as a good candidate for  $\mu\text{LoM}$ .

## ACKNOWLEDGEMENT

Authors want to thanks P.A.P. Nghiem and N. Chauvin from CEA Saclay for the numerous and fruitful discussions about  $\mu\text{LoM}$  and beam dynamics.

## REFERENCES

- [1] J. Knaster *et al.*, “Challenges of the Current Prototype Accelerator of IFMIF/EVEDA”, in *Proc. 7<sup>th</sup> Int. Particle Accelerator Conf. (IPAC’16)*, Busan, South Korea, May 2016, paper MOZB02, pp. 52-57.
- [2] J. Marroncle *et al.*, « IFMIF-LIPAc Diagnostics and its Challenges », in *Proc. Int. Beam Inst. Conf. (IBIC’12)*, Tsukuba, Japan, Oct. 2012, paper WECC01, pp. 557-565
- [3] P. Cara *et al.*, “The Linear IFMIF Prototype Accelerator (LIPAc) Design Development Under The European-Japanese Collaboration”, in *Proc. IPAC’16*, Busan, South Korea, May 2016, paper MOPOY057, pp. 985-988.
- [4] R. Gobin *et al.*, “Installation and first operation of the IFMIF Injector at the Rokkasho site”, in *Proc. ICIS’15*, New York, USA, Aug. 2015, paper MONPS05.
- [5] B. Bolzon *et al.*, “Intermediate Commissioning Result of the 70 mA/50 keV H<sup>+</sup> and 140 mA/100 keV D<sup>+</sup> ECR Injector of IFMIF/LIPAc”, in *Proc. IPAC’16*, Busan, South Korea, May 2016, paper WEPMY033, pp. 2625-2627.
- [6] P. Mereu *et al.*, “Mechanical Integration of the IFMIF-EVEDA Radio Frequency Quadrupole”, in *Proc. IPAC’16*, Busan, South Korea, May 2016, paper THPY025, pp. 3712-3715.
- [7] I. Podadera *et al.*, “RF Design of the Re-buncher Cavities for the LIPAc Deuteron Accelerator”, in *Proc. IPAC’11*, San Sebastian, Spain, Sept. 2011, paper MOPC047, pp. 184-186.
- [8] H. Dzitko *et al.*, “Technical and logistical challenges for IFMIF-LIPAc cryomodule construction, in *Proc. SRF’15*, Whistler, Canada, Set. 2015, paper FRB01, pp. 1453-1459.
- [9] P.A.P. Nghiem *et al.*, *Laser and Particle Beams*, vol. 32, pp. 639-649, 2014.
- [10] P.A.P. Nghiem *et al.*, “Advanced Concepts for Very High Intensity Linacs”, in *Proc. IPAC’16*, Busan, South Korea, May 2016, paper THYA01, pp. 3155-3160.
- [11] N. Chauvin *et al.*, “Halo Matching For High Intensity Linacs and Dedicated Diagnostics”, presented at HB2014, East Lansing, USA, Nov. 2014, paper TUO2AB02, unpublished.
- [12] J. Marroncle *et al.*, “Micro-Loss Detector for IFMIF-EVEDA”, in *Proc. DIPAC’11*, Hamburg, Germany, May 2011, paper MOPD42, pp. 146-148.
- [13] J. Marroncle *et al.*, “ $\mu$ -Loss for LIPAc”, presented in “Cryogenic Beam Loss Monitors Workshop”, <http://indi.co.cern.ch/event/156472/>, Cern, Switzerland, Oct. 2011.
- [14] H. Pernegger *et al.*, “Diamond TCT measurement down to 60 K”, presented in “Cryogenic Beam Loss Monitors Workshop”, <http://indi.co.cern.ch/event/156472/>, Cern, Switzerland, Oct. 2011.
- [15] D. B. Pelowitz, ed., “MCNPX<sup>TM</sup> User’s Manual,” Version 2.5.0, Los Alamos National Laboratory report LA-CP-05-0369, April 2005.
- [16] Cividec, <https://cividec.at/>
- [17] CAEN, <http://www.caen.it/cs/site/Caen-Prod.jsp?idmod=570&parent=11>